Neuroscience Letters 760 (2021) 136081

Contents lists available at ScienceDirect

Neuroscience Letters

journal homepage: www.elsevier.com/locate/neulet

Research article

The integrative role of the M1 in motor sequence learning

Yuki H. Hamano [a,b], Sho K. Sugawara [a,b,c], Masaki Fukunaga [a,b], Norihiro Sadato [a,b,*]

[a] Division of Cerebral Integration, National Institute for Physiological Sciences, Aichi 444-8585, Japan
[b] Department of Physiological Sciences, School of Life Sciences, SOKENDAI (The Graduate University for Advanced Studies), Kanagawa 240-0193, Japan
[c] Neural Prosthesis Project, Department of Dementia and Higher Brain Function, Tokyo Metropolitan Institute of Medical Science, 2-1-6, Kamikitazawa, Setagaya, Tokyo 158-8506, Japan

ARTICLE INFO

Keywords:
Motor learning
Sequential finger tapping
Short-term training
Motor engram
fMRI

ABSTRACT

The primary motor cortex (M1) is crucial in motor learning. Whether the M1 encodes the motor engram for sequential finger tapping formed by an emphasis on speed is still inconclusive. The active states of engrams are hard to discriminate from the motor execution per se. As preparatory activity reflects the upcoming movement parameters, we hypothesized that the retrieval of motor engrams generated by different learning modes is reflected as a learning-related increase in the preparatory activity of the M1. To test this hypothesis, we evaluated the preparatory activity during the learning of sequential finger-tapping with the non-dominant left hand using a 7T functional MRI. Participants alternated between performing a tapping sequence as quickly as possible (maximum mode) or at a constant speed of 2 Hz paced by a sequence-specifying visual cue (constant mode). We found a training-related increase in preparatory activity in the network covering the bilateral anterior intraparietal sulcus and inferior parietal lobule extending to the right M1 during the maximum mode and the right M1 during the constant mode. These findings indicate that the M1, as the last effector of the motor output, integrates the motor engram distributed through the networks despite training mode differences.

1. Introduction

The primary motor cortex (M1) is crucial in motor learning [1]. A recent neuroimaging study showed that M1 encodes integrated spatiotemporal information of learned finger sequences, suggesting that this area holds skill-dependent representations [2]. Human and primate electrophysiological studies also imply that contralateral M1 represents the sequential learned skill [3,4]. Repetitive transcranial magnetic stimulation of the contralateral M1 in humans immediately after training in a ballistic pinch task disrupts skill consolidation during the offline period after practice [3]. Similarly, muscimol injection into the contralateral M1 of non-human primate selectively disrupts the sequential learned behavior [4]. Thus, the M1 is the part of the neural substrates of sequence learning, that is, the engram. Engram refers to a persistent change in the brain by a specific experience [5]. An engram is activated through interaction with retrieval cues (ecphory). An engram exists between the two active encoding and retrieval processes in a dormant state when the synaptic connection's strength is stabilized.

The M1 engagement in fast learning up to 1 h is highly influenced by the specific task and attentional demands [6–8]. However, this influence is not entirely understood. For example, it is unknown if the M1 similarly represents the motor engrams generated by different learning procedures. Previously, Hamano et al. [9] conducted functional MRI with a sequential finger-tapping task by the non-dominant left hand. Participants alternated between performing a tapping sequence as quickly as possible (maximum mode) or at a constant 2 Hz speed, paced by a sequence-specifying visual cue (constant mode). They depicted the dormant state motor engram as a learning-related increase in network centrality during the resting condition by eigenvector centrality (EC) mapping. They found that a network covering the left anterior intraparietal sulcus and inferior parietal lobule represented the engram for execution speed, and the bilateral premotor cortex and right M1 represented the sequential order of movements. They also found a tendency for the dormant engram to increase throughout maximum mode in the right M1. This finding suggests that the M1, as the last effector of the motor output, integrates the motor engrams generated by different training modes during learning [9]. If this notion is correct, the ecphoric state of the engrams in the M1 should increase as learning proceeds. This speculation is partly supported by incrementing the task-related BOLD response during both maximum and constant modes [9]. However, the effect of movement speed on the task-related BOLD response during maximum mode is challenging to differentiate from the retrieval of the

* Corresponding author at: Division of Cerebral Integration, National Institute for Physiological Sciences, Aichi 444-8585, Japan.
E-mail address: sadato@nips.ac.jp (N. Sadato).

https://doi.org/10.1016/j.neulet.2021.136081
Received 14 April 2021; Received in revised form 18 June 2021; Accepted 20 June 2021
Available online 23 June 2021

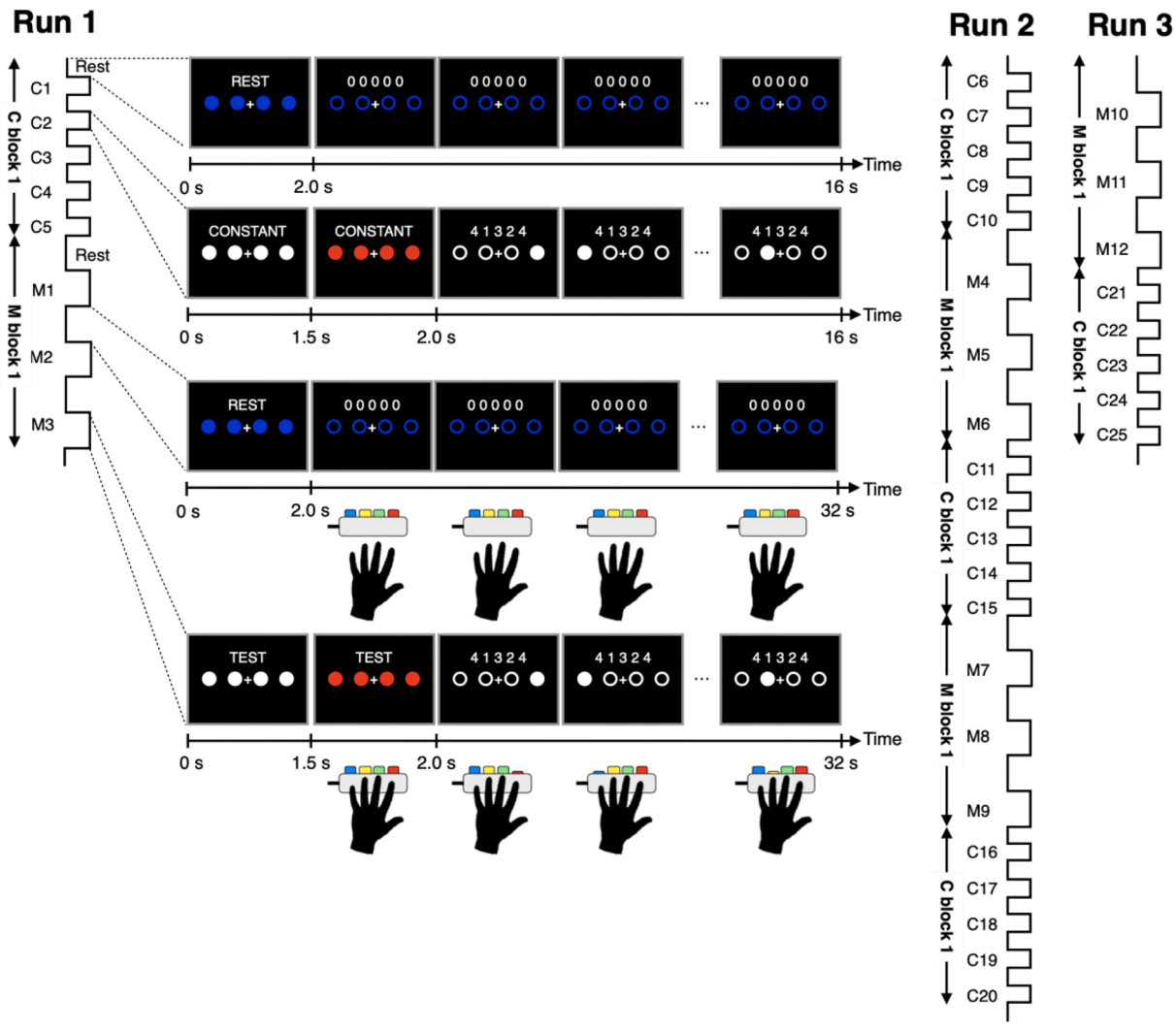

Fig. 1. The task design. The task consisted of constant mode (C1 to C5) and maximum mode (M1 to M3) of sequential finger-tapping learning with the left hand, with the control condition (Rest). Four blue circles were aligned within an equally spaced horizontal array on the screen, corresponding to the left-hand fingers through the buttons' spatial arrangement.

enhanced motor engram (that is, ecphory) from the frequency effect for the execution [10,11]. The frequency effect includes the motor commands that control the finger muscles, corollary discharges, and reafferent feedback from the fingers [12]. Thus, it is necessary to isolate the ecphoric state from the actual execution.

Preparatory activity is known to reflect the parameters of the upcoming movement by non-human primates [13–16], as well as human electroencephalogram (EEG) studies [17–20]. Recently, functional magnetic resonance imaging (fMRI) decoding using machine learning methods [21–24] has made significant contributions to identifying the parameters of upcoming actions represented in the human preparatory activity: Grasp shape [25], reaching direction [26], the effector used for the forthcoming action [27]. Patterns of sequential finger movements [12] were decoded from the preparatory activity in parietal and frontal regions, including the supplementary motor area (SMA), M1, and the dorsal premotor cortex (PMd). Furthermore, freely chosen (internally motivated) grasp shapes can be predicted by the preparatory activity in multiple frontal and parietal brain regions [28]. Hirose et al. [29] have shown that preparatory activity in cortical motor areas represents information about the effector used for an upcoming movement, and those well-formed motor representations are associated with reduced response times. Based on these findings, we hypothesized that the preparatory activity before movement execution includes the ecphoria. To test this hypothesis, we evaluated the preparatory activity during the learning of sequential finger tapping with the non-dominant left hand using 7TMRI. We expected that the motor engram generated by different learning modes is reflected as a learning-related increase in the preparatory activity of the M1.

2. Methods

2.1. Participants

A total of 15 healthy right-handed adult volunteers participated in the study (eight males and seven females; mean age [M ± SD] = 21.87 ± 1.60 years-old) without any overlap with the participants reported in our previous study [9]. Handedness was assessed by the Edinburgh Handedness Inventory [30]. None of the participants had a history of neurological or psychiatric diseases. All participants provided written informed consent for participation in the experiment. The study was conducted according to the Declaration of Helsinki and approved by the Ethical Committee of the National Institute for Physiological Sciences, Japan.

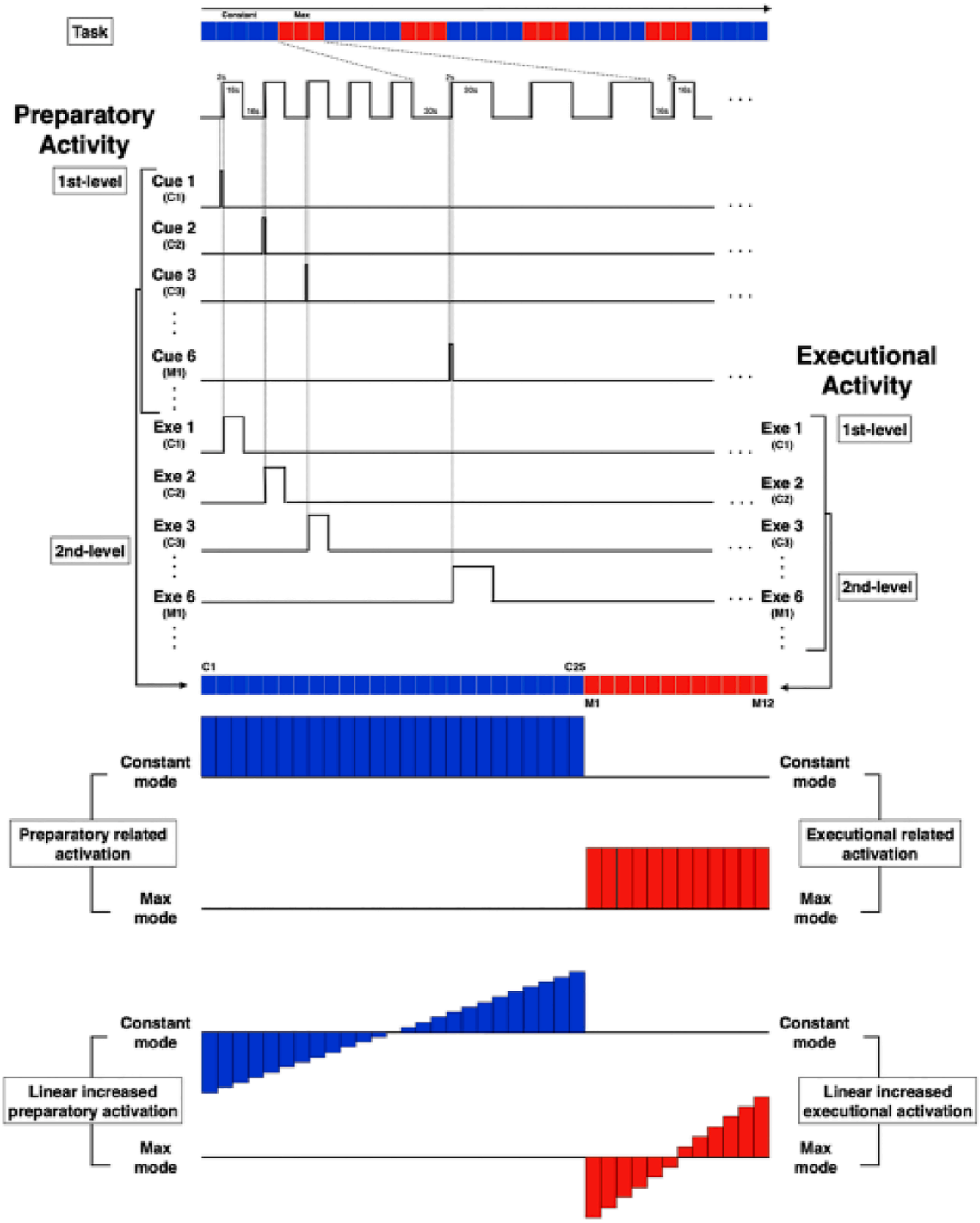

Fig. 2. Scheme of statistical analysis with a general linear model. The parameter estimates of the preparatory activity (left) at an individual level with the general linear model were concatenated into Constant block and Maximum block, preserving each block's temporal order. The concatenated parameter estimates of each participant were incorporated into group-level analysis with a flexible factorial design with predefined contrasts (Bottom). Identical procedures were applied to the execution-related activity (right).

2.2. Experimental procedures

All participants performed a sequential finger-tapping task [9] inside the 7.0T-MRI scanner (Magnetom 7T; Siemens Healthcare GmbH, Erlangen, Germany). They also participated in the resting-state fMRI measurement and the somatotopic representation of the primary somatosensory cortex, both of which will be reported elsewhere. Presentation 12.2 software (Neurobehavioral Systems, Albany, NY, USA) implemented on a personal computer (dc7900; Hewlett-Packard, Palo Alto, CA, USA) was used for stimulus presentation and response time measurements. A digital light processing (DLP) projector (EH503, Optoma, New Taipei City, Taiwan), located outside and behind the scanner, projected stimuli through a waveguide to a translucent screen that the participants viewed via a mirror attached to the head coil of the MRI scanner. The distance between the screen and each participant's eyes was approximately 48 cm, and the angle 5.2° (horizontal) × 3.9° (vertical).

The task procedure followed that previously reported [9]. There

were three fMRI runs. The first (Run 1) consisted of a block of constant mode (C block) followed by a block of maximum mode (M block). C block (Fig. 1), 2 min 40 s in duration, started with a Rest epoch of 16-sec duration followed by a constant mode epoch of 16 sec, alternatively repeated five times. The Rest epoch began with the instruction phase. With the message of "Rest," four blue filled circles aligned with an equally spaced horizontal array corresponding to the left-hand fingers (from left to right, small, ring, middle, and index fingers) appeared on the screen for 2000 ms (Fig. 1). For the remaining duration (14 s), the message of "0 0 0 0 0" and four blue open circles appeared on the screen. After 16 sec of rest epoch, the Constant epoch, where participants were asked to respond by pressing the button indicated by the white circle, started with the display of the instruction. In the instruction display, the message of "CONSTANT" and four white filled circles appeared on the screen for 1500 ms. Then, the circles' color changed to red for 500 ms, followed the execution phase for 14 sec. One of the rings was filled in every 500 ms in the execution phase, indicating the tapping fingers and buttons on an MR-compatible button box (Current Design, Philadelphia, USA). A sequence composed of a five-element series, either "index (4) – little (1) – middle (3) – ring (2) – index (4)" (presented to 8 participants) or "ring (2) – index (4) – middle (3) – little (1) –ring (2)" (presented to the other 7 participants). The frequency of the color and location change was 2 Hz. The sequence of "4-1-3-2-4" or "2-4-3-1-2" appeared on the upper side of the screen during the execution phase as a reminder. The Constant epoch lasted 16 s when alternated with the Rest epoch. Rest and Constant epochs alternated five times, constituting C block 1. M block 1 (Fig. 1), 3 min in duration, started with a Rest epoch identical to the C block except that it lasted 30 s instead of 16 s. Similar to the Constant epoch, the Maximum epoch started with the instruction phase. In the instruction phase, the message of "TEST" and four white filled circles appeared on the screen for 1500 ms to ask the participant to tap the memorized sequence as rapidly and accurately as possible. Then the color of the circles changed to red for 500 ms. After the offset of the red circles, the participants started pressing buttons. Visual feedback of correct tapping was provided by moving the white filled circle to the next position. If the participant made an incorrect response, the filled circle remained at the previous position until the correct button was pressed. The Maximum epoch lasted 30 s. Rest and Maximum epochs were conducted alternatively three times following the previous fMRI studies [31,32].

The second run (Run 2) consisted of three C blocks separated by two M blocks, and the third run (Run 3) started with one M block followed by a C block. Overall, the sequential finger task in this study was built with five C blocks (a total of 13 min 20 s) and four M blocks (12 min), presented in alternation (Fig. 1).

2.3. Behavioral analysis

The performance was measured by speed and accuracy. Transition time (in ms) was defined as the mean time between two correct button responses per epoch. The error rate was the number of error responses among all responses per epoch. Because the behavioral task consisted of several blocks, including three or five epochs each (Fig. 2), we dissociated the between-block effect and within-block effect for performance changes in both constant and maximum modes. For each performance measure (i.e., transition time and error rate in each mode [constant or maximum]), a repeated-measures analysis of variance (rmANOVA) was conducted with task epoch and task block as independent variables. All statistical analyses were performed using R version 3.6.1 statistical software (http://cran.us.r-project.org), and the level of significance was $p < 0.05$.

2.4. MRI data acquisition

Each participant's head was immobilized within a 32-element phased array head coil and 1-ch transmitter head coil. fMRI was performed using a multiband Gradient-Echo Echo Planar Image (GE-EPI) sequence [33](echo time [TE] = 25 ms, repetition time [TR] = 2000 ms; field of view [FOV] = 192 × 192 mm^2; flip angle = 65°; matrix size = 160 × 160; 120 slices; slice thickness = 1.2 mm; multiband factor = 4, GRAPPA = 3, Phase partial Fourier = 6/8). To measure the B0 field for EPI distortion correction, two spin echo EPI images with reversed phase encoding directions were acquired (TR/TE = 7700/60 ms; FOV = 192 × 192 mm^2; FA = 78°; matrix size = 160 × 160; 120 slices; slice thickness = 1.2 mm, Phase partial Fourier = 6/8).

We also scanned a series of structural images from all participants on another day with 3TMRI (Magnetom Verio; Siemens Ltd., Erlangen, Germany) to correct the distortion of 7T EPI due to static field inhomogeneity and non-linearity of gradient [34]. Two separate of T1-weighted (T1w) and T2-weighted (T2w) images were acquired using 3D magnetization-prepared rapid-acquisition gradient echo sequence (MPRAGE; [35] TR = 2400 ms; TE = 2.24 ms; FOV = 256 mm × 240 mm; flip angle = 8°; matrix size = 320 × 320; slice thickness = 0.8 mm; 224 sagittal slices; GRAPPA = 2) and the variable flip angle turbo spin-echo sequence (Siemens SPACE; Mugler et al., 2000; TR = 3200 ms; TE = 560 ms; FOV = 256 × 240 mm^2; matrix size = 320 × 320; slice thickness = 0.8 mm; 224 sagittal slices; GRAPPA = 2), respectively. Similar to the functional MRI session, two spin echo EPI images with reversed phase encoding directions were acquired (TR = 7700; TE = 60 ms; FOV = 192 × 192 mm^2; FA = 78°/160°; matrix size = 98 × 98; 72 slices; slice thickness = 2 mm, phase partial Fourier = 6/8).

2.5. MRI data preprocessing

To investigate the group-averaged task-related activity, we normalized functional images from native space into standard space. To correct the distortion of functional images measured by 7T-MRI, we adopted the minimal preprocessing pipelines [36] developed for the Human Connectome Project (HCP; [37]) [34]. HCP-style preprocessing was constituted from structural and functional pipelines. Although HCP-style preprocessing includes surface-based processing, we only used volume-based processing. We applied the structural pipeline to T1w and T2w images. First, image distortions resulting from gradient non-linearity were corrected. After the brain region was extracted, readout distortions were corrected using the field map generated from two spin-echo EPIs with opposite phase-encoding directions and a Topup toolbox ([38]). Un-distorted T1w and T2w images were registered with cross-modal boundary-based registration (BBR; [39]). Because the intensity of T1w and T2w images still had biases, bias field correction was applied to un-distorted images. Finally, we estimated the nonlinear registration matrix from native space to MNI template space and applied this nonlinear registration to T1w and T2w images.

The functional pipeline also started by correcting gradient non-linearity and readout distortions. To correct head motion, EPIs were registered into single-band reference (SBRef) EPI, scanned at the first of each session by estimating six parameters of rigid-body transformation from each EPI to SBRef EPI. In this study, we conducted structural and functional MRI sessions on different days. Thus, we calculated the session-specific field map from two Spin Echo (SE)-EPIs measured in functional MRI sessions. With this field map, we applied readout distortion correction to motion-corrected EPIs using the Topup toolbox. The transformation matrix from SBRef EPI to T1w image was estimated by BBR cross-modal registration method. Then, this BBR parameter was applied to undistorted EPIs to register all EPIs into the T1w image. The resulted EPIs were transformed into MNI template space using T1w-to-MNI parameters estimated in structural pipelines. Finally, the image intensities of EPIs were normalized to the 4D whole-brain mean of 10,000 (arbitrary grayscale value). The normalized functional images were spatially smoothed using a Gaussian kernel of 5 mm full width at half maximum (FWHM) in the x, y, and z axes.

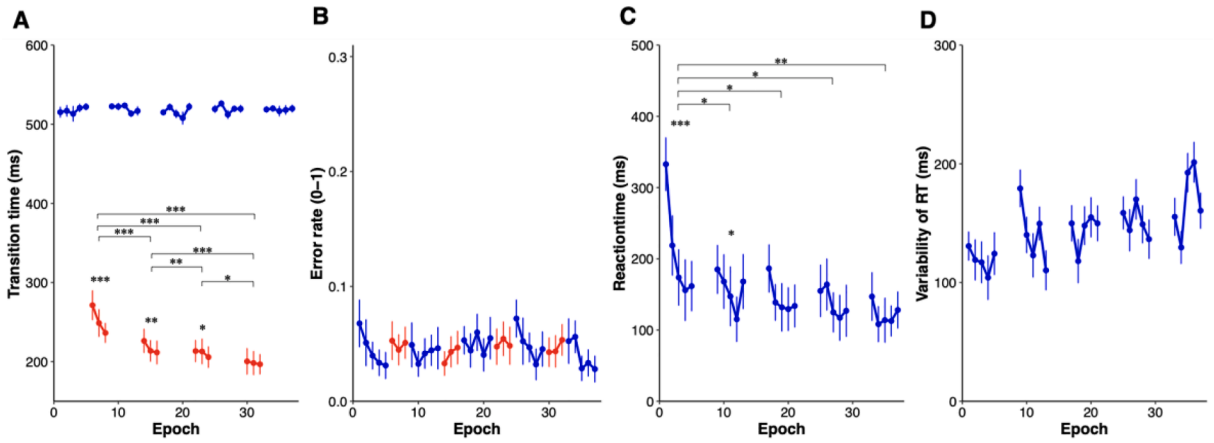

Fig. 3. Performance in maximum mode (red) and constant mode (blue). (A) The transition time between button presses, (B) error rates, (C) reaction time between cue and button press, and (D) the variability (standard deviation) of reaction time. Data points represent group means for each epoch, and error bars indicate the standard error of the mean. *$p < .05$, **$p < .01$, ***$p < .001$ (rmANOVA).

2.6. Functional MRI data analyses

We analyzed the task-related activity with Statistical Parametric Mapping software (SPM12; The Welcome Trust Center for Neuroimaging) in MATLAB 2018a. The first five volumes of each fMRI run were discarded because of unsteady signal. Statistical analysis of the fMRI data was conducted at two levels. At the first level, a general linear model (GLM) was fitted to the fMRI data for each participant [40,41]. Each task epoch was divided into an instruction event and execution phase to depict the preparatory activity and the execution-related activity separately. Each instruction event was modeled with a stick function: the onset was specified at the beginning of the instruction cue presentation with 0 duration. Each motor execution epoch was modeled with a boxcar function, with the onset specified at the beginning of the execution with 30-sec duration for maximum mode and 12-s duration for constant mode. The orthogonality of the consecutive stick function and boxcar function was confirmed. The first and third runs include five constant mode epochs and three maximum mode epochs, while the second run included 15 constant mode epochs and six maximum mode epochs. Thus, a total of 37 instruction events and 37 execution phases were modeled in GLM. All regressors were convolved with the canonical hemodynamic response function. Also, to consider the effect of head motions, six motion parameters were contained in GLM. The time series for each voxel was high-pass filtered at 1/128 Hz. For advanced rapid sampling techniques such as the multi-band GE-EPI used in this study, a first-order autoregressive model does not sufficiently capture temporal correlations in time series with higher sampling rates [42]. Thus, the "FAST" model implemented in SPM12 was applied to adequately address the temporal correlations in time series with higher sampling rates [43] for data whitening. Then, to calculate the estimated parameters, a least-squares estimation was performed on the high-pass filtered and pre-whitened data.

The parameter estimates for each regressor in each "contrast" image were submitted to second-level analysis [44] with a flexible-factorial model that incorporated within-participant factors of 'Repetition' and 'Mode' (constant/maximum). Predefined contrasts for each mode were applied to depict preparatory activity related to task-cue in each speed mode. Furthermore, to investigate changes in the preparatory activity related to learning of the sequential finger-tapping skill, predefined linearly increasing contrast for each mode was estimated. Increasing contrast vectors were defined numerically as an increment of 1 per each task-cue, keeping the mean equal to zero. The resulting set of voxel values for each contrast constituted the statistical parametric mapping of t value, SPM{t}. The statistical threshold for the spatial extent test on the clusters, defined by the height threshold of $p < 0.001$, was set at $p < 0.05$, corrected for family-wise error [45], except otherwise specified.

3. Results

3.1. Performance

To test the between-block and within-block changes of behavioral performance with the acquisition of a sequential finger-tapping skill, we evaluated transition time and error rate during maximum mode (red closed circle, Fig. 3A, B). Transition time exhibited a significant effect of block (two-way rmANOVA, $F(3,42) = 83.45$, $p < .001$, $\eta^2_G = 0.11$), epoch ($F(2,28) = 12.70$, $p < .001$, $\eta^2_G = 0.013$) and their interaction ($F(6,84) = 5.20$, $p = .0024$, $\eta^2_G = 0.0087$). Simple main effect of epoch showed the significant reduction of transition time in M1 (one-way rmANOVA, $F(2,28) = 12.26$, $p < .001$), M2 ($F(2,28) = 8.85$, $p = .0015$), and M3 ($F(2,28) = 3.56$, $p = .048$). According to post-hoc between-block comparisons, mean transition time decreased from M1 to M2 (paired *t* test, $t(14) = 8.85$, $p < .001$), M2 to M3 ($t(14) = 2.74$, $p = .016$), and M3 to M4 ($t(14) = 4.03$, $p < .0025$). Error rate did not exhibit any significant effect of block (two-way rmANOVA, $F(3,42) = 1.04$, $p = .37$, $\eta^2_G = 0.0048$), epoch ($F(2,28) = 2.22$, $p = .13$, $\eta^2_G = 0.0021$), and their interaction ($F(6,84) = 1.18$, $p = .33$, $\eta^2_G = 0.0050$).

Performance in constant mode was evaluated by the reaction time from presentation of the visual cue to tapping (Fig. 3C). The block effect (two-way rmANOVA, $F(4, 56) = 9.74$, $p < .001$, $\eta^2_G = 0.0052$), epoch effect ($F(4, 56) = 12.30$, $p < .001$, $\eta^2_G = 0.014$), and their interaction ($F(16, 224) = 4.15$, $p = .001$, $\eta^2_G = 0.029$) were significant. Simple main effect of epoch showed the significant reduction of transition time in C1 (one-way rmANOVA, $F(4,56) = 19.46$, $p < .001$) and C2 ($F(4,56) = 4.22$, $p = .013$). According to post-hoc between-block comparisons, mean transition time decreased from C1 to C2 (paired *t* test, $t(14) = 3.76$, $p = .002$), but not from C2 to C3 ($t(14) = 0.80$, $p = .43$), C3 to C4 ($t(14) = 0.51$, $p = .87$), and C4 to C5 ($t(14) = 0.21$, $p = .68$). For the variability of reaction time in terms of standard deviation, neither the block effect (two-way rmANOVA, $F(4, 56) = 1.02$, $p = .39$, $\eta^2_G = 0.0053$), epoch effect ($F(4, 56) = 1.51$, $p = .24$, $\eta^2_G = 0.0076$), nor their interaction ($F(16, 224) = 1.40$, $p = .22$, $\eta^2_G = 0.014$) was significant (Fig. 3D). These findings indicated that both maximum and constant modes enhanced performance.

3.2. Execution-related activation

Both maximum mode and constant mode showed a similar activation pattern in the left Cerebellum, the right M1, and the bilateral PMd extending to PMv, SMA/pre-SMA, and the dorsal inferior parietal lobule

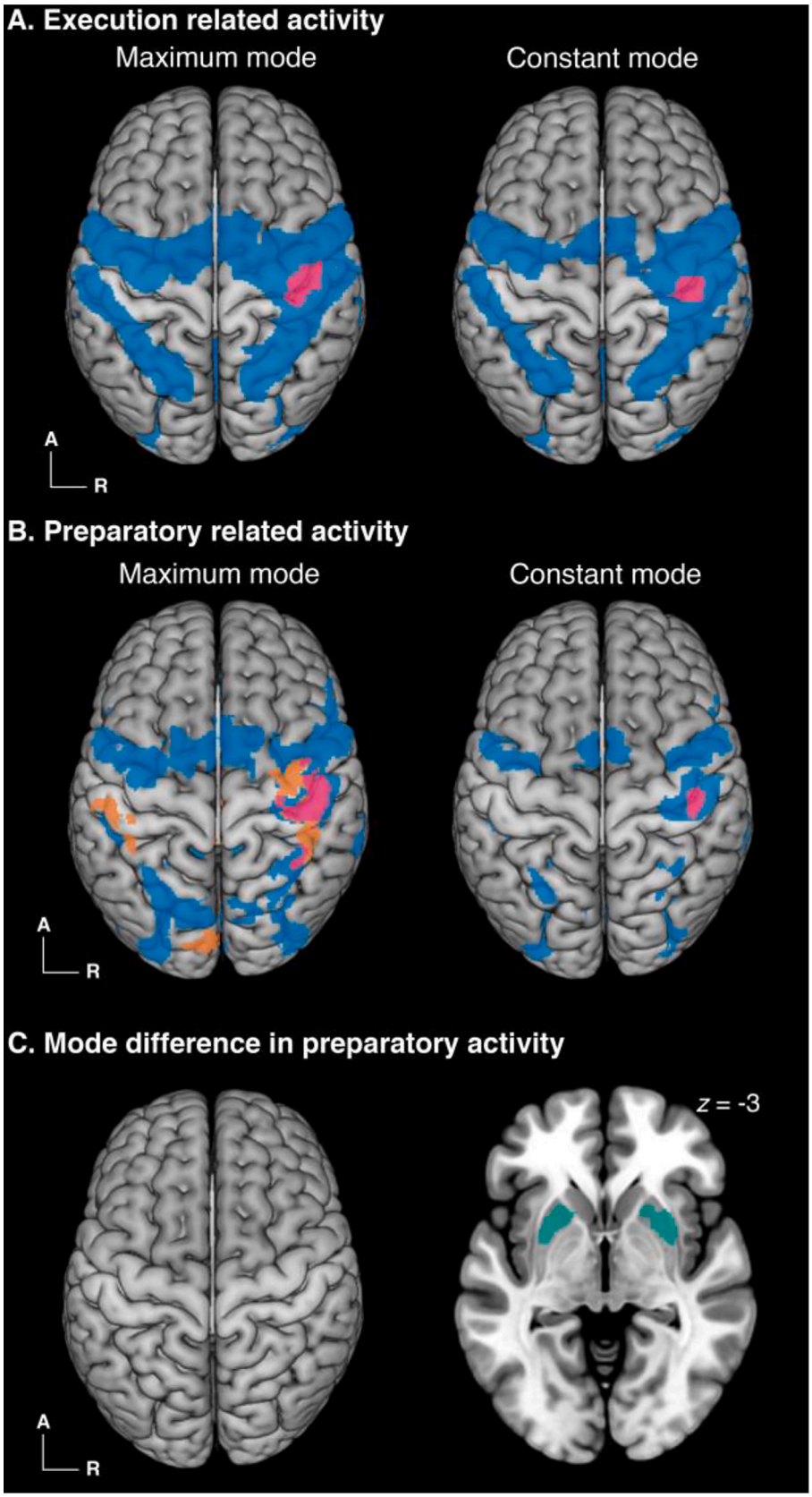

Fig. 4. Task-related activation. (A) Execution-related activities (blue) overlap with their linear increase (magenta) of maximum mode (left) and constant mode (right) superimposed on surface rendered high resolution MRI. $P < 0.05$ corrected at the cluster level. (B) Preparatory activities (blue), linear increase (orange), and overlap (magenta) of maximum mode (left) and constant mode (right) with the same format and statistical threshold as A. (C) Mode difference in preparatory activation. Conjunction analysis between the contrast of mode subtraction (Maximum > Constant) and maximum mode activity during the preparation period (green). $P < 0.05$ corrected at the peak level.

(dIPL) extending to the anterior IPL (aIPL), and the visual cortex. An increment of the activation was found in the right M1 in both max and constant mode (Fig. 4A).

3.3. Preparation-related activation

Both maximum and constant mode showed the preparation-related activity in the right M1, bilateral PMd extending to the PMv, SMA/pre-SMA, the dIPL extending to the aIPL, and the visual cortex. No cerebellar activation was found (Fig. 4B). Bilateral putamen showed maximum mode-specific activation (Fig. 4C). A linear increase of the preparatory activity was found in the right M1, bilateral intraparietal sulcus (IPS) region, and the visual cortices during the max mode and the right M1 during the constant mode (Fig. 4B).

4. Discussion

4.1. Preparation-related activation similar to execution-related activation

We found a common preparation-related activity in the areas activated by execution of fine motor control, that is, the M1, PMv, PMd, and IPL, in maximum and constant modes.

These areas are known to be involved in the control of fine hand movement [46]. As the present study utilized the same sequence for both maximum and constant modes, these areas represent the sequential finger movement irrespective of the execution mode; internally generated vs. externally guided or maximum speed vs. constant speed.

4.2. Learning-related preparatory activation

4.2.1. Constant mode

The present study first showed that the start-cue-related preparatory activation of the right M1 prior to the constant mode finger movement increased as learning proceeded. As we have previously demonstrated, the motor engram of the constant mode appeared in the M1 [2]. This finding is consistent with our hypothesis that the preparatory activity is the retrieved motor engram, that is, ecphory.

4.2.2. Maximum mode

Furthermore, we showed that the start-cue-related preparatory activation of the right M1 increased as learning proceeds during maximum mode (magenta in Fig. 4B left). This finding supports our hypothesis that the engrams of the sequential finger movements formed by the different learning modes are commonly represented in the M1. Previous non-human primate studies described the cells in the M1 that show the anticipatory activity of the specifically memorized sequence of upcoming movements [4]. Recently, inhibition of protein synthesis in the M1 of the non-human primate was shown to disrupt the maintenance of the sequential finger movement engram [47]. As both learning modes deal with an identical motor sequence, the present finding indicates that the M1 is related to the sequence's engram. Thus, the M1, as the last effector of the motor output, integrates the motor engram distributed through the networks despite training mode differences.

Also, a learning-related increment of the preparatory activation of the left anterior intraparietal sulcus (aIPS) coincides with the previous finding [9] of distinct motor engrams in this area. In the last study by Hamano et al. [9], during the maximum mode, EC during rest significantly increased in the left aIPS as learning proceeded, and this EC was enhanced by task execution. They argued that the enhanced EC in the aIPS represented the accumulation of information related to the body reference frame provided by comparing prediction and feedback during execution, thus specific to the maximum mode learning. Halsband and Lange [48] argued that the right IPL during initial motor learning is attributed to integrating sensory information and feedback processing. In contrast, the left counterpart represents the acquired skill within a body-reference frame. Present findings suggest that the right M1, at the time of engram retrieval before the maximum mode execution, integrates distinct motor engrams located in a different region, the left aIPS.

4.2.3. Constant preparatory activation specific to maximum mode

The movement mode difference is reflected in the preparatory activity. The preparation-related activity before the bilateral striatum's maximum mode was constantly more prominent than that before the constant mode. This finding may be related to the difference between the self-paced, internally driven movement in the maximum mode and cued movement in the constant mode. Maximum mode explicitly required the retrieval of predefined sequences, thus internally generated from memory, whereas constant mode did not. An electrophysiological study of non-human primates [49] showed that self-timed movement, compared with cued movement, showed a slow build-up of activity before movement initiation, which may drive movement initiation by increasing until exceeding an activity threshold. A human neuroimaging study also showed that internally generated action plans are related to the pre-movement activities of the frontostriatal networks [50]. The authors argued that the striatum is related to planning the entire sequences, whereas, during movement, subroutines for individual movements are implemented. This finding suggests that the constant preparatory activity is more prominent for self-paced, internally generated movement than for externally cued action, representing the motor plan retrieval for execution initiation.

4.2.4. Explicit learning

In the present study, the same sequence was learned by both modes, and was, thus, explicit learning. However, during the maximum mode, the participants had to retrieve the sequence from memory to initiate the movement. They also had to try to execute the sequence as fast and accurately as possible. Therefore, during the maximum mode, the participants conducted the self-timed movement, explicitly monitoring the ongoing procedure with the preceded trials in terms of speed and accuracy. On the other hand, the constant mode required the tapping finger indicated by the visual cue, and therefore, triggered movement without the need for explicit retrieval of the sequence nor performance monitoring.

Previous electrophysiological [51] and neuroimaging [52] studies showed the involvement of the M1 for implicit sequence learning and by explicit learning. Implicit learning, as measured as a shortening of the reaction time, was represented by the increased task-related activity of the M1. In contrast, explicit learning, shown as a positive correlation with the correct recall of the sequence, was associated with increased activity in the fronto-parietal cortex [52]. Combined with previous studies, including ours [9], the present study indicates that the learning mode difference in sequence learning is reflected in the neural pathways' difference for generating the motor engram out of the M1. The maximum mode involves the parietal cortices, whereas the constant mode includes the premotor cortices [9]. Both processes end up with integrated engram formation in the M1, as the last effector for sequence execution.

5. Conclusion

Using enhanced preparatory activity as a retrieved motor engram's measure, we successfully depicted an early-phase engram of sequential finger-tapping formed in the M1 irrespective of the learning modes.

CRediT authorship contribution statement

Yuki H. Hamano: Investigation, Formal analysis, Writing - original draft. **Sho K. Sugawara:** Investigation, Formal analysis, Visualization. **Masaki Fukunaga:** Resources, Validation. **Norihiro Sadato:** Conceptualization, Writing - review & editing, Funding acquisition, Supervision.

Acknowledgements

This study was supported, in part, by Grants-in-Aid for Scientific Research #15H01846 (to N.S.), #15K21602 and #18K13378 (to S.K.S.), #19K22985 (to M.F.) and #20K19629 (to Y.H.H.) from the Japan Society for the Promotion of Science, and by the Strategic Research Program for Brain Sciences from the Japan Agency for Medical Research and Development (AMED) under grant number JP18dm0107152. The authors have no conflicts of interest or financial disclosures to report. We would like to thank Dr. Hans-Peter Fautz, Dr. Tobias Kober, Dr. Tim DeVito, Dr. Josef Pfeuffer, Saurabh Shah, Andreas Greiser and Thomas Banner (Siemens Healthineers GmbH) for providing the sequences of pre-scanning adjustment on 7T MRI.

References

[1] J. Dupont-Hadwen, S. Bestmann, C.J. Stagg, Motor training modulates intracortical inhibitory dynamics in motor cortex during movement preparation, Brain Stimul. 12 (2019) 300–308, https://doi.org/10.1016/j.brs.2018.11.002.

[2] K. Kornysheva, J. Diedrichsen, Human premotor areas parse sequences into their spatial and temporal features, Elife 3 (2014), e03043, https://doi.org/10.7554/eLife.03043.

[3] W. Muellbacher, U. Ziemann, J. Wissel, N. Dang, M. Kofler, S. Facchini, B. Boroojerdi, W. Poewe, M. Hallett, Early consolidation in human primary motor cortex, Nature 415 (2002) 640–644, https://doi.org/10.1038/nature712.

[4] X. Lu, J. Ashe, Anticipatory activity in primary motor cortex codes memorized movement sequences, Neuron 45 (2005) 967–973, https://doi.org/10.1016/j.neuron.2005.01.036.

[5] S.A. Josselyn, S. Köhler, P.W. Frankland, Finding the engram, Nat. Rev. Neurosci. 16 (2015) 521–534, https://doi.org/10.1038/nrn4000.

[6] E. Hazeltine, S.T. Grafton, R. Ivry, Attention and stimulus characteristics determine the locus of motor-sequence encoding. A PET study, Brain 120 (1997) 123–140, https://doi.org/10.1093/brain/120.1.123.

[7] K. Stefan, M. Wycislo, J. Classen, Modulation of associative human motor cortical plasticity by attention, J. Neurophysiol. 92 (2004) 66–72, https://doi.org/10.1152/jn.00383.2003.

[8] E. Dayan, L.G. Cohen, Neuroplasticity subserving motor skill learning, Neuron 72 (2011) 443–454, https://doi.org/10.1016/j.neuron.2011.10.008.

[9] Y.H. Hamano, S.K. Sugawara, T. Yoshimoto, N. Sadato, The motor engram as a dynamic change of the cortical network during early sequence learning: An fMRI study, Neurosci. Res. 153 (2020) 27–39, https://doi.org/10.1016/j.neures.2019.03.004.

[10] N. Sadato, V. Ibañez, M.P. Deiber, G. Campbell, M. Leonardo, M. Hallett, Frequency-dependent changes of regional cerebral blood flow during finger movements, J. Cereb. Blood Flow Metab. 16 (1996) 23–33, https://doi.org/10.1097/00004647-199601000-00003.

[11] N. Sadato, V. Ibanez, G. Campbell, M.-P.-P. Deiber, D. Le Bihan, M. Hallett, V. Ibañez, G. Campbell, M.-P.-P. Deiber, D. Le Bihan, M. Hallett, Frequency-dependent changes of regional cerebral blood flow during finger movements: functional MRI compared to PET, J. Cereb. Blood Flow Metab. 17 (1997) 670–679, https://doi.org/10.1097/00004647-199706000-00008.

[12] I. Nambu, N. Hagura, S. Hirose, Y. Wada, M. Kawato, E. Naito, Decoding sequential finger movements from preparatory activity in higher-order motor regions: A functional magnetic resonance imaging multi-voxel pattern analysis, Eur. J. Neurosci. 42 (2015) 2851–2859, https://doi.org/10.1111/ejn.13063.

[13] E.V. Evarts, J. Tanji, Reflex and intended responses in motor cortex pyramidal tract neurons of monkey, J. Neurophysiol. 39 (1976) 1069–1080, https://doi.org/10.1152/jn.1976.39.5.1069.

[14] J. Tanji, E.V. Evarts, Anticipatory activity of motor cortex neurons in relation to direction of an intended movement, J. Neurophysiol. 39 (1976) 1062–1068, https://doi.org/10.1152/jn.1976.39.5.1062.

[15] M. Godschalk, R.N. Lemon, H.G.T. Nijs, H.G.J.M. Kuypers, Behaviour of neurons in monkey peri-arcuate and precentral cortex before and during visually guided arm and hand movements, Exp. Brain Res. 44 (1981) 113–116, https://doi.org/10.1007/BF00238755.

[16] J. Tanji, K. Taniguchi, T. Saga, Supplementary motor area: Neuronal response to motor instructions, J. Neurophysiol. 43 (1980) 60–68, https://doi.org/10.1152/jn.1980.43.1.60.

[17] H.H. Kornhuber, L. Deecke, Brain potential changes in voluntary and passive movements in humans: readiness potential and reafferent potentials, Pflugers Arch. Eur. J. Physiol. 468 (2016) 1115–1124, https://doi.org/10.1007/s00424-016-1852-3.

[18] H. Shibasaki, G. Barrett, E. Halliday, A.M. Halliday, Components of the movement-related cortical potential and their scalp topography, Electroencephalogr. Clin. Neurophysiol. 49 (1980) 213–226.

[19] B. Libet, C.A. Gleason, E.W. Wright, D.K. Pearl, Time of conscious intention to act in relation to onset of cerebral activity (readiness-potential): The unconscious initiation of a freely voluntary act, Brain. 106 (1983) 623–642, https://doi.org/10.1093/brain/106.3.623.

[20] H. Shibasaki, M. Hallett, What is the Bereitschaftspotential? Clin. Neurophysiol. 117 (2006) 2341–2356, https://doi.org/10.1016/j.clinph.2006.04.025.

[21] J.D. Haynes, G. Rees, Decoding mental states from brain activity in humans, Nat. Rev. Neurosci. 7 (2006) 523–534, https://doi.org/10.1038/nrn1931.

[22] K.A. Norman, S.M. Polyn, G.J. Detre, J.V. Haxby, Beyond mind-reading: multi-voxel pattern analysis of fMRI data, Trends Cogn. Sci. 10 (2006) 424–430, https://doi.org/10.1016/j.tics.2006.07.005.

[23] E. Formisano, F. De Martino, G. Valente, Multivariate analysis of fMRI time series: classification and regression of brain responses using machine learning, Magn. Reson. Imaging 26 (2008) 921–934.

[24] F. Pereira, T. Mitchell, M. Botvinick, Machine learning classifiers and fMRI: a tutorial overview, Neuroimage 45 (2009) S199–S209, https://doi.org/10.1016/j.neuroimage.2008.11.007.

[25] J.P. Gallivan, D.A. McLean, K.F. Valyear, C.E. Pettypiece, J.C. Culham, Decoding action intentions from preparatory brain activity in human parieto-frontal networks, J. Neurosci. 31 (2011) 9599–9610, https://doi.org/10.1523/JNEUROSCI.0080-11.2011.

[26] J.P. Gallivan, D. Adam McLean, F.W. Smith, J.C. Culham, Decoding effector-dependent and effector-independent movement intentions from human parieto-frontal brain activity, J. Neurosci. 31 (2011) 17149–17168, https://doi.org/10.1523/JNEUROSCI.1058-11.2011.

[27] J.P. Gallivan, D.A. McLean, J.R. Flanagan, J.C. Culham, Where one hand meets the other: Limb-specific and action-dependent movement plans decoded from preparatory signals in single human frontoparietal brain areas, J. Neurosci. 33 (2013) 1991–2008, https://doi.org/10.1523/JNEUROSCI.0541-12.2013.

[28] G. Ariani, M.F. Wurm, A. Lingnau, Decoding internally and externally driven movement plans, J. Neurosci. 35 (2015) 14160–14171, https://doi.org/10.1523/JNEUROSCI.0596-15.2015.

[29] S. Hirose, I. Nambu, E. Naito, Cortical activation associated with motor preparation can be used to predict the freely chosen effector of an upcoming movement and reflects response time: An fMRI decoding study, Neuroimage 183 (2018) 584–596, https://doi.org/10.1016/j.neuroimage.2018.08.060.

[30] R.C.C. Oldfield, The assessment and analysis of handedness: The Edinburgh inventory, Neuropsychologia 9 (1971) 97–113, https://doi.org/10.1016/0028-3932(71)90067-4.

[31] M.P. Walker, T. Brakefield, A. Morgan, J.A. Hobson, R. Stickgold, Practice with sleep makes perfect: Sleep-dependent motor skill learning, Neuron 35 (2002) 205–211, https://doi.org/10.1016/S0896-6273(02)00746-8.

[32] M.P. Walker, T. Brakefield, J.A. Hobson, R. Stickgold, Dissociable stages of human memory consolidation and reconsolidation, Nature 425 (2003) 616–620, https://doi.org/10.1038/nature01951.1.

[33] S. Moeller, E. Yacoub, C.A. Olman, E. Auerbach, J. Strupp, N. Harel, K. Uğurbil, Multiband multislice GE-EPI at 7 tesla, with 16-fold acceleration using partial parallel imaging with application to high spatial and temporal whole-brain FMRI, Magn. Reson. Med. 63 (2010) 1144–1153, https://doi.org/10.1002/mrm.22361.

[34] T. Yamamoto, M. Fukunaga, S.K. Sugawara, Y.H. Hamano, S. Norihiro, Quantitative evaluations of geometrical distortion corrections in cortical surface-based analysis of high-resolution functional MRI data at 7 Tesla, J. Magn. Roson. Imaging 53 (2021) 1220–1234.

[35] J.P. Mugler, J.R. Brookeman, Three-dimensional magnetization-prepared rapid gradient-echo imaging (3D MP RAGE), Magn. Reson. Med. 15 (1990) 152–157, https://doi.org/10.1002/mrm.1910150117.

[36] M.F. Glasser, S.N. Sotiropoulos, J.A. Wilson, T.S. Coalson, B. Fischl, J.L. Andersson, J. Xu, S. Jbabdi, M. Webster, J.R. Polimeni, D.C. Van Essen, M. Jenkinson, The minimal preprocessing pipelines for the Human Connectome Project, Neuroimage 80 (2013) 105–124, https://doi.org/10.1016/j.neuroimage.2013.04.127.

[37] M.F. Glasser, T.S. Coalson, E.C. Robinson, C.D. Hacker, J. Harwell, E. Yacoub, K. Ugurbil, J. Andersson, C.F. Beckmann, M. Jenkinson, S.M. Smith, D.C. Van Essen, A multi-modal parcellation of human cerebral cortex, Nature 536 (2016) 171–178, https://doi.org/10.1038/nature18933.

[38] J.L.R. Andersson, S. Skare, J. Ashburner, How to correct susceptibility distortions in spin-echo echo-planar images: Application to diffusion tensor imaging, Neuroimage 20 (2003) 870–888, https://doi.org/10.1016/S1053-8119(03)00336-7.

[39] D.N. Greve, B. Fischl, Accurate and robust brain image alignment using boundary-based registration, Neuroimage 48 (2009) 63–72, https://doi.org/10.1016/j.neuroimage.2009.06.060.

[40] K.J. Friston, P. Jezzard, R. Turner, Analysis of functional MRI time-series, Hum. Brain Mapp. 1 (1994) 153–171, https://doi.org/10.1002/hbm.460010207.

[41] K.J.J. Worsley, K.J.J. Friston, Analysis of fMRI time-series revisited—again, Neuroimage 2 (1995) 173–181, https://doi.org/10.1006/nimg.1995.1023.

[42] S. Bollmann, A.M. Puckett, R. Cunnington, M. Barth, Serial correlations in single-subject fMRI with sub-second TR, Neuroimage 166 (2018) 152–166, https://doi.org/10.1016/j.neuroimage.2017.10.043.

[43] N. Corbin, N. Todd, K.J. Friston, M.F. Callaghan, Accurate modeling of temporal correlations in rapidly sampled fMRI time series, Hum. Brain Mapp. 39 (2018) 3884–3897, https://doi.org/10.1002/hbm.24218.

[44] A.P. Holmes, K.J. Friston, Generalisability, random effects and population inference, Neuroimage 7 (1998) S754.

[45] K.J. Friston, A. Holmes, J.-B. Poline, C.J. Price, C.D. Frith, Detecting activations in pet and fMRI: levels of inference and power, Neuroimage 4 (1996) 223–235, https://doi.org/10.1006/nimg.1996.0074.

[46] S.H.I. Merchant, E. Frangos, J. Parker, M. Bradson, T. Wu, F. Vial-Undurraga, G. Leodori, M.C. Bushnell, S.G. Horovitz, M. Hallett, T. Popa, The role of the inferior parietal lobule in writer's cramp, Brain 143 (2020) 1766–1779, https://doi.org/10.1093/brain/awaa138.

[47] M. Ohbayashi, Inhibition of protein synthesis in M1 of monkeys disrupts performance of sequential movements guided by memory, Elife 9 (2020) 1–12, https://doi.org/10.7554/eLife.53038.
[48] U. Halsband, R.K. Lange, Motor learning in man: A review of functional and clinical studies, J. Physiol. Paris 99 (2006) 414–424, https://doi.org/10.1016/j.jphysparis.2006.03.007.
[49] I.H. Lee, J.A. Assad, Putaminal activity for simple reactions or self-timed movements, J. Neurophysiol. 89 (2003) 2528–2537, https://doi.org/10.1152/jn.01055.2002.
[50] C.L. Elsinger, D.L. Harrington, S.M. Rao, From preparation to online control: Reappraisal of neural circuitry mediating internally generated and externally guided actions, Neuroimage 31 (2006) 1177–1187, https://doi.org/10.1016/j.neuroimage.2006.01.041.
[51] A. Pascual-Leone, J. Grafman, M. Hallett, Modulation of cortical motor output maps during development of implicit and explicit knowledge, Science (80-.) 263 (1994) 1287–1289.
[52] M. Honda, M.P. Deiber, V. Ibáñez, A. Pascual-Leone, P. Zhuang, M. Hallett, Dynamic cortical involvement in implicit and explicit motor sequence learning. A PET study, Brain 121 (1998) 2159–2173, https://doi.org/10.1093/brain/121.11.2159.